Earth and Planetary Science Letters 365 (2013) 51–62

Contents lists available at SciVerse ScienceDirect

Earth and Planetary Science Letters

journal homepage: www.elsevier.com/locate/epsl

Stable isotope fractionation by thermal diffusion through partially molten wet and dry silicate rocks

I.N. Bindeman [a,*], C.C. Lundstrom [b], C. Bopp [b], F. Huang [b,c]

[a] Department of Geological Sciences, 1272 University of Oregon, Eugene, OR 97403, USA
[b] Department of Geology, University of Illinois, Urbana, IL 61801, USA
[c] CAS Key Laboratory of Crust-Mantle Materials and Environments, School of Earth and Space Sciences, University of Science and Technology of China, Hefei 230026, China

ARTICLE INFO

Article history:
Received 12 January 2012
Received in revised form
26 December 2012
Accepted 27 December 2012
Editor: T.M. Harrison
Available online 15 February 2013

Keywords:
thermal diffusion
hydrogen isotope separation
oxygen isotopes
lithium isotopes
17-O
meteoric hydrothermal systems

ABSTRACT

Water plays a fundamental role in affecting geochemical transport and physical properties of magmas. Here we show the previously undocumented behavior of water within partially molten silicate resting in a temperature gradient, producing O, Li and H isotope redistribution by thermal diffusion leading to enrichment of light isotopes at the hot end of the gradient. After weeks to months, fully molten as well as mostly crystalline portions of water-bearing experiments develop remarkably large isotope and chemical redistributions: up to 28‰ for $\delta^{18}O$, 144‰ for δD, and 18‰ for $\delta^{7}Li$. In contrast, long-term dry experiments develop smaller ($\sim$5‰ $\delta^{18}O$) isotopic fractionations only in the hotter end where it is molten or partially molten. Isotope fractionation of oxygen is linearly related to temperature, and the magnitude of isotopic separation per °C is $\sim 2\times$ larger for wet experiments than dry ones. We explain this by water de-polymerizing the silicate structure leading to a smaller size of diffusing SiO*x* fragments. The magnitude of isotope separation between the hot and cold ends for Li, Mg, Fe, O, and H isotopes increases linearly with $\Delta M_{heavy-light}/M_{light}$. These relationships provide predictive tests for natural rocks and highlight the role of water in isotope and compositional redistribution during temperature gradient mediated processes. We discuss the implications to natural environments in which the lightest stable isotopes (H, Li, O) with the greatest $\Delta M_{heavy-light}/M_{light}$ and fastest diffusion coefficients are capable of achieving mass-dependent redistribution in a transient temperature gradient. These experiments underscore the importance of solution–reprecipitation in wet subsolidus systems and demonstrate that isotopic redistribution can be established $\sim$6 orders of magnitude quicker than by diffusion through a traditional silicate melt at higher temperature. This has important implications for timescales of natural isotope and chemical redistribution by thermal diffusion.

1. Introduction

1.1. Water and temperature gradients

Water is the component in silicate melts having the greatest impact on melt structure, mineral–melt equilibrium, diffusive transport properties, and melt viscosity. Because Earth is a unique planetary body in our solar system having both liquid H_2O and a granitic crust, water has been inferred to be the primary reason for the existence of Earth's continental crust (Barth, 1962; Campbell and Taylor, 1983).

Coexisting crystalline solids and fluids (melt or hydrous solution) lying within a temperature gradient characterize many igneous and metamorphic environments. Yet the role of temperature gradients in compositional differentiation of magmas has been questioned ever since Bowen's (1921) work showed that diffusive heat loss was orders of magnitude faster than diffusion of mass. However, present observations from plutons indicate this reasoning may be oversimplified, leaving open the role of temperature gradients in magmatic differentiation, especially in hydrous contact aureols on small or large scale. The duration of time required to maintain temperature gradients is often cited as negative evidence against the possibility of temperature gradient-based effects in nature. However, if transport of atoms between hot and cold end is accelerated by the presence of water (or by transport through interconnected water films) then effects may be more pronounced (e.g. Idlefonse and Gabis, 1973). Importantly, the sense of isotope redistribution by temperature gradient (light at hot-end and heavy at the cold end) is often opposite to the sense expected for chemical diffusion (Huang et al., 2009; Lundstrom, 2009), and this provides a test to recognize such effects in nature.

Here we show a here-to-fore-unrecognized behavior of wet silicate materials in a temperature gradient. Specifically, we report results from a stable isotopic investigation of H, Li, and O in five piston cylinder experiments involving dry basalt and wet andesite and rhyolites starting materials, held in a temperature gradient from

* Corresponding author. Tel.: +1 5413463817.
E-mail address: bindeman@uoregon.edu (I.N. Bindeman).

0012-821X/$ - see front matter © 2013 Elsevier B.V. All rights reserved.
http://dx.doi.org/10.1016/j.epsl.2012.12.037

7 to 66 days. While all experiments reflected the thermal migration process whereby diffusive redistribution occurred within coexisting minerals and melt, only the wet experiments produced large and systematic isotope ratio variations throughout an entire experiment (Table 1), and only the wet experiments differentiated throughout compositionally. Furthermore, because isotope separations at the cold end of wet experiments occurred at subsolidus temperatures, they provide lower bounds on the rate of isotopic redistribution by wet thermal diffusion processes, encompassing P–T ranges of hydrothermal and metamorphic environments.

1.2. Historical and theoretical background on thermal diffusion

The past 100 years have seen considerable development of theory and experiments aimed at uncovering the role of temperature gradients in mass redistribution. Enskog (1911) provided the first

Table 1
Stable isotope ratios and water contents in experimental charges.

Distance, median (interval) (mm)	T (°C)	Lithology, minerals	$\delta^{18}O$ ‰	D/H ‰	H_2O wt%	$\delta^{7}Li$ ‰	1SD ‰	Li ppm	$\delta^{56}Fe$ ‰	$\delta^{26}Mg$ ‰
Andesite, wet, AGV experiment, 66 days										
17.75 (17.5–18)	952	gl	−4.79						−1.644	−8.34
13.5 (12–15)	936	gl	−4.35	−127.2	7.02	−2.4	0.14	82	−0.91	−6.5
10.1 (9.2–11)	902	gl+cr, Amph 45%	−0.06	−102.3	3.56				1.12	1.53
9.3	889	gl+cr, Amph 42%	0.86							
8.8	880	gl+cr, Amph 19%	2.35	−105.3	2.58					
6.2	811	cr, Bi 15%	4.69	14.7	0.72				0.08	−0.57
3.2	685	cr, Bi 12%	9.02	16.1	0.73	16.1	0.28	12		
1.6 (0−3.2)	591	cr, Bi 9%	12.7	17.4	0.49				0.07	−0.6
0.5	515	cr, Bi 6%	13.62							
0 (−0.5 to 0.5)	411	cr, Qz 80–100%	18.4							
Omega, permil/100°/amu			2.065	43		7.36			0.383	1.37
Rhyolite, wet, RGM experiment, 25 days										
10.25	912	gl								
9.5 (9–10)	904	gl	−5.91		5.81					
8.75 (8.5–9)	896	gl	−4.76							
8	888	gl			5.58					
7.5	875	gl	−3.08		4.96					
7	865	gl			2.87					
6.25 (6–6.5)	840	gl+cr	−1.19							
5.5 (5–6)	812	gl+cr, Ms, <5%	0.64		0.36					
4.75 (4.5–5)	776	cr, Ms, 10%	1.80		0.56					
3.25 (2.5–4)	682	cr, Ms, 20–50%	11.76		1.60					
2.25	587	cr, Ms, 20–50%			2.01					
1.5	512	cr, Ms, 20–50%			1.71					
0.5 (0–1)	416	cr	22.44							
Omega, permil/100°/amu			2.94							
Rhyolite, wet, MA1 experiment, 10 days, not at steady state										
Distance (for H_2O and D/H)										
0.5	395	cr, Qz > 80%	15.96	−168.5	1.32	0.75				
1.25	458	cr, Qz+Ms	12.13	−161.8	1.17	2.75				
3.5	617	cr, Plag 20–50%	8.74							
5.2	710	cr	2.09	−158.8	1.23	5.5				
6.2	755	cr	−2.31	−163.1	1.50	6.3				
7.2	794	cr	5.79	−160.6	1.57	8				
9.7	867	gl+cr	6.67	−140.1	0.63	8.8				
9	850	gl	6.55	−109.0	0.19	9.8				
11	893	gl	6.67	−98.98	0.39	10.8				
12	908	gl	6.75	−100.87	0.41	12.5				
13	920	gl	6.73	−109.1	2.30	14.75				
15.25	936	gl	7.03	−99.78	3.36	15.5				
Basalt, dry, LTB experiment, 34 days										
6.1	1261	gl	3.48							
4.6	1189	gl	7.76							
3.3	1105	gl+cr	8.59							
1.5	957	cr	8.46							
0.0	803	cr	8.23							
Omega, permil/100°/amu			1.60							
Basalt, dry, STB experiment, 7days										
8.75	1246	gl	7.15							
7.25	1166	gl	7.09							
6.5	1118	gl+cr	7.09							
5.75	1063	cr	7.06							
4.25	934	cr	7.25							
1.5	619	cr	7.31							
0	400	cr	7.09							

Comments: Uncertainty of $\delta^{18}O$ measurements is 0.09‰, except in LTB experiment where due to small sample size it is estimated to be between 0.1‰ and 0.25‰. Uncertainties on δD are 1.5‰, water is 0.05 wt%. Omega parameters for AGV and RGM experiments were calculated from best fit slopes of $\delta^{18}O$ and δD vs. T; in LTB experiment only molten portion was used to calculate Omega. For Li and previously published Fe and Mg isotopes (Huang et al., 2009) isotopic difference between most contrasting values were used. The triple-oxygen $\Delta^{17}O$ measurements were performed on tops and bottoms of AGV experiment and are mass-dependent within ±0.19‰, 2stdev uncertainty on garnet standards: AGV top (glass): $\Delta^{17}O = +0.04$‰, AGV-bottom (powder) = −0.18‰; AGV starting powder = −0.08‰, when the $\Delta^{17}O$ is defined as $\delta^{17}O - 0.52\delta^{18}O$. See Appendix for analytical details.

theoretical treatment of thermal diffusion (diffusion driven by a temperature gradient) in gases by adding the role of temperature gradients to simple kinetic theory. Light isotopes and light elements accumulated in the hot end in accordance with cross-flux Onsager's (1931) reciprocal rule of non-equilibrium thermodynamics. Thermal diffusion in flowing gas was used as one of the methods of isotope separation and enrichment for industrial applications (Grew and Ibbs, 1952; Vasaru et al., 1969). Soret (1879) provided observations of the separation of salt solutions put in a temperature gradient. The significant compositional rearrangement observed in this effect led some geologists to suggest it might cause large scale differentiation in silicic magma bodies (Hildreth, 1981). This prompted experiments on supra-liquidus silicate melts by Walker and DeLong (1982) and Lesher and Walker (1986, 1991) (for clarity, these are referred to as "Soret experiments" here) that indeed showed significant compositional redistribution due to the temperature gradient effect. Notably, Lesher and Walker (1991) showed that the compositional trends in Soret experiments were largely opposite to those observed in silicic magma bodies (hot: higher Si, Na; cold: higher Mg, Ca, Fe), thus ruling out a supra-liquidus temperature gradient process as a viable magma differentiation mechanism.

However, Lesher and Walker (1988) and Walker et al. (1988) also performed temperature gradient experiments at lower overall temperature in which silicate melt and minerals coexisted, referred to as "thermal migration" experiments (after Buchwatd et al., 1985). Compositional trends in these experiments behave distinctly from Soret experiments as melt compositions are dictated by mineral–melt equilibrium at a given temperature and by different saturation temperatures for different minerals. Importantly, all previous thermal migration experiments were performed anhydrous. Huang et al. (2009) described thermal migration experiments in which water was added to andesite powder placed in a gradient from 950 °C to 350 °C. In experiment AGV lasting 66 days and further described and studied below, the original andesitic starting material compositionally rearranged to form a granitic bulk composition at the cold-end of the gradient, and evolved into zones variably enriched in different hydrous minerals. Simulations using the IRIDIUM program (Boudreau, 2003) reproduce the general mineralogical distribution in the experiment, suggesting that the thermal migration differentiation process follows expectations of mineral–melt or mineral–fluid equilibria.

Thermal diffusion results in large isotopic fractionations in both liquids and gases with lighter isotopes always being preferentially enriched at the hot end of the gradient. Kyser et al. (1998) provided the first demonstration of thermal diffusion isotopic fractionation in silicate melts showing a systematic change in $\delta^{18}O$ over a range of silicate melt compositions. The $\delta^{18}O$ fractionation in these experiments can be quantified by the thermal diffusion isotopic sensitivity (Ω: ‰/100 °C/amu) with Ω ranging from 1.2 to 1.4. More recent studies (Richter et al., 2008, 2009; Huang et al., 2010) show large fractionations of Mg, Si, Ca and Fe in other silicate melt Soret experiments. Notably, the hotter, melt-rich region the AGV experiment of the Huang et al. (2009), thermal migration experiment produced Ω_{Mg} and Ω_{Fe} identical to those found in the Soret experiments despite the presence of coexisting minerals. No fractionation from the starting Mg and Fe isotope ratios was observed in the lower half of this experiment which was almost entirely solid.

The theory behind the temperature gradient isotopic effect is incomplete (Richter et al., 2009; Dominguez et al., 2011; Lacks et al., 2012). The multi-phase experiments presented in this study may seem fairly complex to interpret, but the regular and rather simple mass-dependent behavior that we observe for isotopes of different elements allows us to put theoretical constraints on redistribution of isotopes of these elements in a temperature field, and emphasize the critical role of water (and transport vis water-bearing fluids) in isotopic redistribution.

2. Methods, experimental and analytical protocols

2.1. General experimental design and description of individual experiments

Five of the thermal migration experiments presented in this work involved placing a starting material powder into a capsule within the imposed temperature gradient of the piston cylinder apparatus for 7–66 days at 0.5 GPa pressure (Figs. 1 and 2, Tables 1 and 2 and Appendix A). Run products consisted of an upper hot portion of 100% glass, a middle region of coexisting minerals and glass, and a lower portion consisting of a fine grained mineral aggregate with no resolvable glass.

2.1.1. LTM-AGV

This experiment reflects thermal migration of a natural andesite rock powder (USGS standard AGV-1) with 4 wt% water added to the internal Au_{75}–Pd_{25} capsule. The experimental conditions and subsequent material characterization were extensively documented in

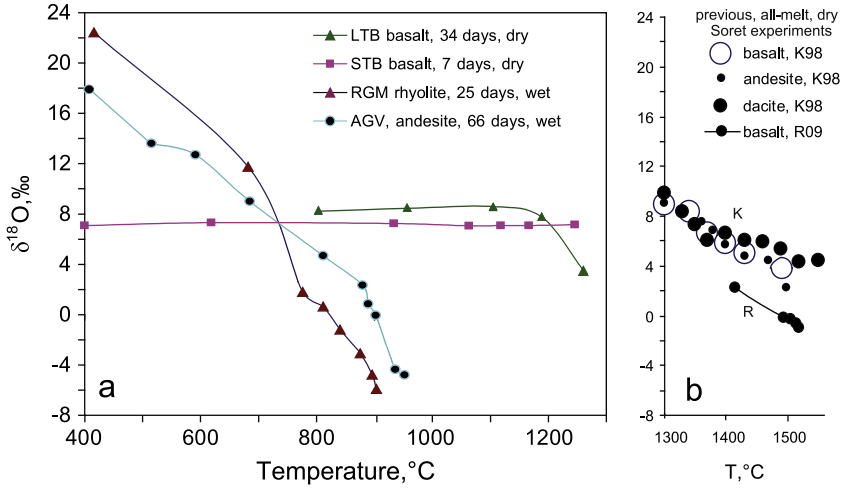

Fig. 1. (a) Thermal diffusion fractionation profile of $\delta^{18}O$ vs. temperature for two water bearing and two nominally anhydrous experiments described in this study. (b) Previously published results of nominally anhydrous experiments Kyser et al. (1998; K98) and Richter et al. (2009; R09). Notice that water bearing experiments developed ~2× greater isotopic fractionation than nominally anhydrous ones; see Table 1 for data.

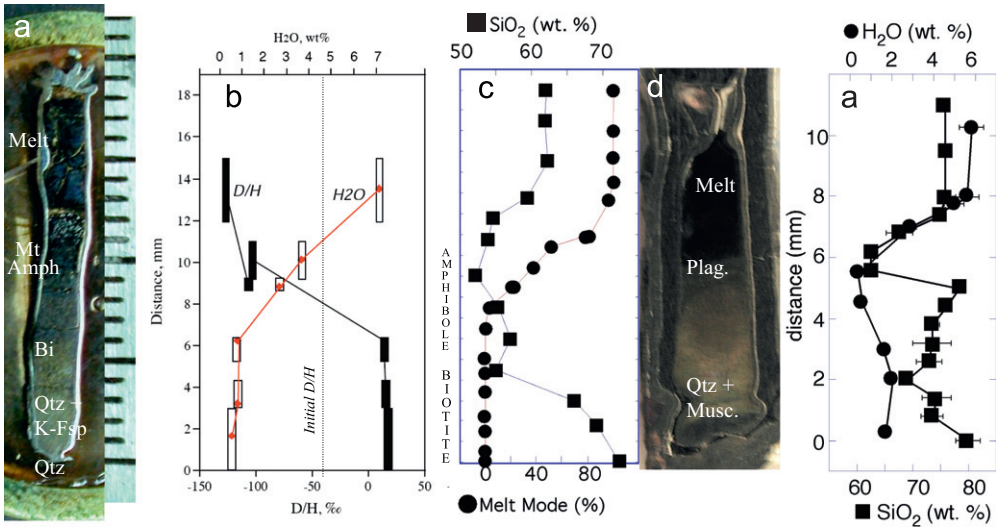

Fig. 2. Microphotographs and details of isotopic and compositional redistribution in LTM-AGV (andesite) and RGM (rhyolite) experiments. (a) reflected light image of AGV experiment; scale bar in mm at right. (b) D/H and H_2O content, measured by TCEA, (c) melt mode and SiO_2 as function of position, (d) reflected light image of RGM experiment (scale corresponds to Y axis in e), (e) H_2O and bulk silica content with position for RGM experiment.

Huang et al. (2009); a brief description of this experiment is given here. A 2 cm long inner Au_{75}–Pd_{25} capsule, sealed inside a thick walled Pt capsule, was held with the hot end at 950 °C and cold end at 350 °C for 66 days. The outer capsule contained $CoCl_2$ as a H_2 getter, leading to full retention of water during the duration of this experiment based on SIMS analyses (Huang et al., 2009). The water distribution and retention of H during the experiment is confirmed here by TCEA water content analysis and hydrogen isotopic mass balance. After 66 days, the originally homogeneous starting material compositionally differentiated into a fully molten upper third, a middle third composed of a melt–amphibole–plagioclase aggregate and a lower third composed of a fine grained almost completely crystalline solid having a granitic bulk composition.

A new finding from this experiment was the discovery of a ~1.5 mm thick layer of almost pure quartz along the very bottom of the capsule in this experiment. In the process of regrinding and repolishing the charge, we observed that the previous polishing had not actually reached the bottom of the capsule. To our surprise, X-ray mapping revealed a region of almost pure quartz with only a few crystals of K-spar, muscovite and an unidentified Mg–K–Al–Fe–Si phase (the phase is too rich in Al and Si to be solely biotite but could be a mixture of biotite and other phase; Supplementary Fig. A4). After imaging and bulk analysis, we extracted a chip of material from this region and measured it for $\delta^{18}O$.

The melt in this experiment remained water-undersaturated. The ~7 wt% water in the melt at the hot end is below ~9.9 wt% water expected for water saturation in a dacitic–andesitic melt at 0.5 GPa (calculated using MELTS, Ghiorso and Sack, 1995). Thus, the large compositional change and transport through the colder portion of the experiment are interpreted to reflect the presence of a fluid phase throughout the experiment having a continuum of compositions from a standard andesitic melt with 7 wt% dissolved H_2O content at the hot end to a small amount of water-rich peralkaline silicate melt at < 400 °C at the cold end (Huang et al., 2009; Lundstrom, 2009).

2.1.2. RGM-1 experiment

Like LTM-AGV, this experiment involved sealing a USGS rock standard powder (rhyolite from Glass Mountain: RGM-1) with ~4 wt% water into a $Au_{75}Pd_{25}$ capsule which was itself sealed into a thick walled Pt capsule with a graphite liner and $CoCl_2$ (see Huang et al., 2009). The experiment was run in a 3/4 in. piston cylinder apparatus but in a smaller (thinner) pressure vessel resulting in a steeper temperature gradient. The run was taken to 0.5 GPa pressure, then ramped up to its hot spot temperature of 900 °C. The temperature at the cold end of this experiment was estimated to be 416 °C. The experiment lasted 25 days followed by turning the power off to the furnace resulting in the temperature dropping hundreds of degrees in a few seconds. The silicate material was removed from the capsule, sectioned and made into a surface mount with chips of the other symmetrical half of the capsule taken for $\delta^{18}O$ analysis. 1024 × 1024 pixel X-ray images were collected to cover the surface area of the charge (Fig. A5) using the JEOL 840A SEM at UIUC. Two area maps, approximately 0.06–0.08 mm^2 in size and at the same horizontal (isothermal) location in the capsule, were chosen for extracting quantitative information on bulk compositions.

Like LTM-AGV, the RGM experiment differentiated into several discrete zones: the upper third of the experiment reflected a fully molten section; this sharply transitioned into a 2 mm thick layer almost entirely composed of plagioclase. Below this, a layer of aggregated silicic minerals (K-feldspar, quartz) and melt followed by an area of mostly K-feldspar. Finally, the bottom of the experiment consisted of quartz plus muscovite. The RGM experiment has undergone large amounts of compositional reorganization dictated by mineral saturation at different temperatures. This results in a general layering with smooth compositional changes and a bottom portion dominated by quartz (and lesser amounts of muscovite) with bulk composition being > 80 wt% SiO_2. Horizontal layering makes up the majority of the exposed surface of the capsule, but the mineral distribution along one side shows a region of larger crystals composed of quartz and K-feldspar.[1]

2.1.3. MA-1 experiment

This short 10 day-long experiment, using a dried naturally-hydrous powdered glass (~1.95 wt% H_2O, $\delta D = -145‰$, Nolan and

[1] The cause of this feature is not known; one possibility is that it represents a significant radial temperature gradient along one side of the capsule. Because the same mineral assemblage covers considerable vertical space in the charge, this explanation seems unlikely. Radial temperature gradients may be slightly non-uniform (Watson et al., 2002; Watson and Price, 2002) but probably cannot account for this feature. A second speculative explanation is that this feature reflects an instability in the transport process forming a conduit along the side of the capsule. The large grain size and euhedral crystal faces pointing to the center of this "conduit-like" feature would be consistent with this explanation although the exact cause remains unknown.

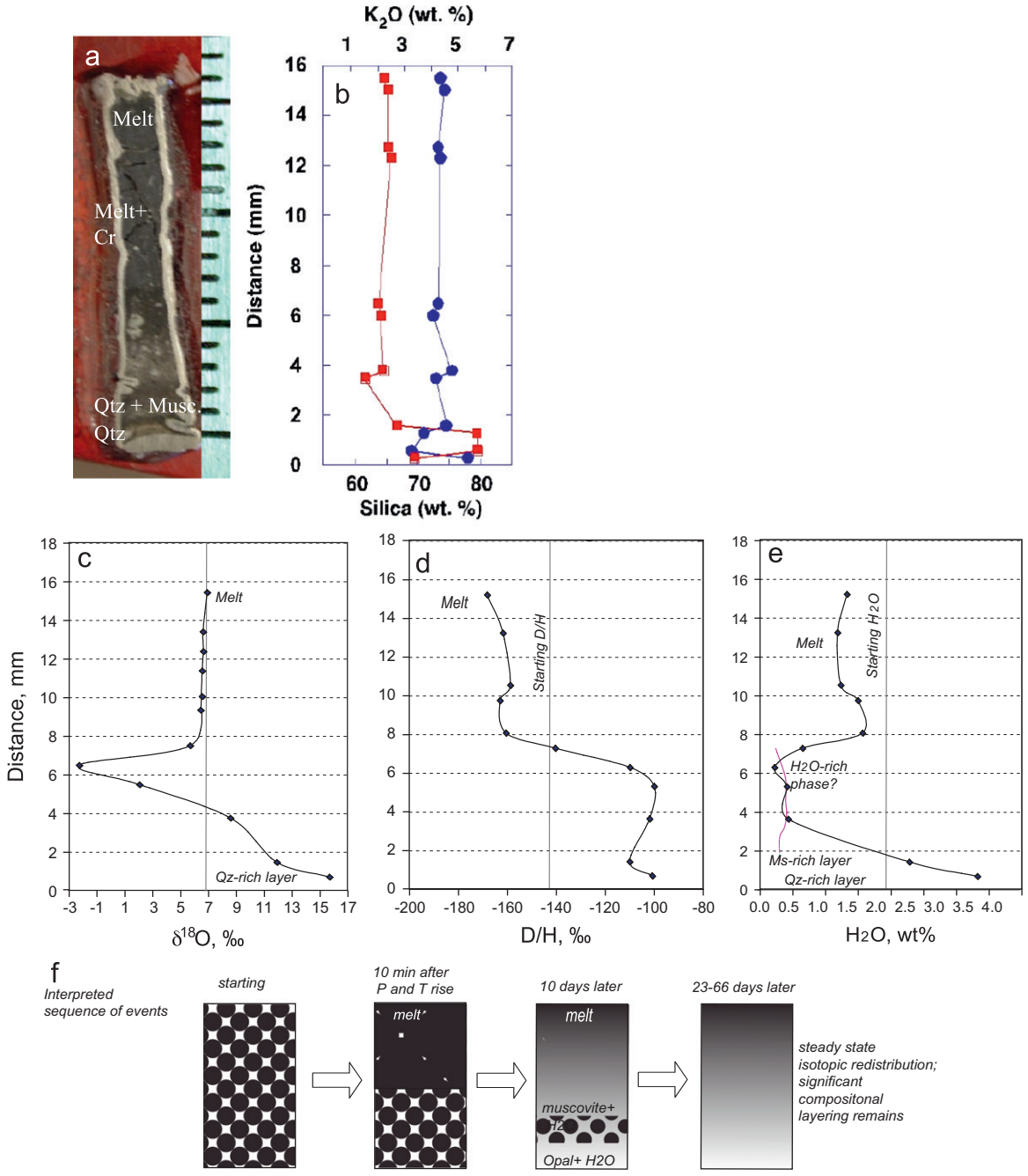

Fig. 3. Microphotograph (a) and details of compositional (b), isotopic (c and d), and $[H_2O]_{tot}$ redistribution in short-term, 10 day-long experiment with Mt Mazama ash run at 5kbars total pressure in a temperature gradient (Table 1). Note the prominent layering developed at the cold end, and K-rich (muscovite) and Si-rich (quartz) areas at the bottom in (b). (c–e) Notice that in this experiment isotopic steady state is not achieved and only the water-saturated cold-end of the capsule, exhibit significant isotopic change with distance, explained by thermal migration through an intergranular fluid phase. The hot end of the experiment represents homogeneous $\delta^{18}O$ values, close in composition to the initial value, consistent with the slower rise time of thermal diffusion in silicate melt (e.g. dry basalt run). The integration of the δD isotope profile shows mass balance with the initial δD value of the hydrous ash, suggesting no hydrogen loss through the walls of the capsule; diffusive water or hydrogen loss would result in severe (hundreds of permil) δD enrichment (as in experiments of e.g. Richet et al., 1986, or our RGM experiment, whose inner AuPd capsule leaked) which is NOT observed in this experiment. Hydrogen isotopic redistribution is 70‰, and the shape is concordant with $\delta^{18}O$ and H_2O_{tot} profiles; the sense of redistribution is consistent with the thermal migration (light at the hot end and heavy at the cold end). Slightly lower than expected total water concentrations found in the hot end of the experiment is explained by the initial water redistribution in a temperature gradient upon temperature rise, mass balance require water to remain in a subsolidus end of the capsule serving as intergranular fluid media for thermal migration and compositional change, leading to significant recrystallization and mineralogical change. Water was lost upon opening of the capsule and sample preparation. The details of the observed distribution of water in the solid and glass products can be explained by the variable proportion of hydrous phases—e.g. muscovite layer (14–16 mm), transitioning to the highest silica content bottom where some opal (20% H_2O) may have remained. to lower concentration of H_2O is due to muscovite being substituted by K—feldspar (9–13 mm).

Bindeman, in press) of Mt. Mazama ash (MA1, Fig. 3), had 2 purposes. First, it differed from the other hydrous experiments because the water was initially dissolved in the glass; and second, this shorter experiment showed the temporal (transient) evolution of mineralogical and isotopic changes, for comparison with longer-duration hydrous experiments above. In MA1 experiment, rapid heating of the rhyolitic bulk composition at the hot end led to the movement of ~0.4 wt% H_2O water from the hot end to the middle and cold end. Like in the longer-duration experiments, the starting glass at the cold end evolved into prominant layers (Ms-rich region and a Qz- and

H_2O-rich at the bottom) with variable proportions of each phase (Fig. 3). The melt+crystals part of the experiment has developed significant compositional, $\delta^{18}O$ and δD changes throughout, while the molten part is close but not identical to the original and record transient change especially in δD which got lowered by ~20‰.

2.1.4. Dry basalt experiments

These involved filling graphite capsules with a starting powder consisting of BCR-1 (USGS standard rock powder made from Columbia River Basalt) with several trace elements added. The two experiments described here were identical except for the period of time they remained at high temperature (7-day STB, 34-day LTB) and slightly different lengths of capsule/placements within the piston cylinder temperature gradient (Table 1, see Bopp (2010) for detailed mineralogical observations from these experiments). The top portions of both experiments were glassy, the middle consisted of minerals coexisting with glass (quenched melt) and the bottoms fine grained material was relatively similar in composition to the starting material. Very little differentiation occurred in the cold subslidus part of experiment. The prominent minerals in the middle portion of the experiment were orthopyroxene, garnet, clinopyroxene and ilmenite. Comparison of the time series of experiments shows that the all melt top portion expands with time, consistent with previous studies (Lesher and Walker, 1991). Although the order of appearance of minerals with temperature is the same between experiments, the longer duration experiment shows prominent grain growth and sorting into discrete mineral layers relative to the short experiment. In the long duration experiment, a monomineralic layer of orthopyroxene ends in a region with large euhedral garnets. The garnets contain a single horizontal layer of ilmenite passing through them. At lower temperatures, large clinopyroxene crystals appear which transitions to the unreacted region previously mentioned.

2.2. Analytical methods

The $^{18}O/^{16}O$ and D/H ratios were analyzed on small chips (0.5–1 mm in dimension) extracted from different spatial positions in each experiment, and the isotopic measurements (Table 1) were performed in the stable isotope lab at the University of Oregon using a home-built laser fluorination system attached to a Finnigan MAT253 mass spectrometer (for $\delta^{18}O$), and by thermal decomposition (TCEA) continuous flow system (for δD and $[H2O]_{tot}$, see Bindeman, 2008, 2012 and Appendix for detailed description of analytical protocols). Given high sensitivity of the MAT253 instrument, the 0.4–1.5 mg of available experimental material was sufficient for analyses of both isotopes with good precision (0.09‰ for $\delta^{18}O$; 1–3‰ for δD). Triple oxygen (for $\Delta^{17}O$ parameter) isotopic measurements relied on ~2 mg and double freezing on 13A mol sieves, and O_2 gas as analyte. δ^7Li was measured at the University of Maryland on dissolved chips (~1 mg) from opposite ends of LTM-AGV by MC-ICP-MS using established methods (Teng et al., 2009). $\delta^{56}Fe$ and $\delta^{26}Mg$ quoted in this work for LTM-AGV are taken from Huang et al. (2009).

3. Isotopic results

3.1. Dry experiments with basalts

The 7-day STB experiment resulted in lack of any measurable redistribution of oxygen isotopes even in the molten upper third of the charge (Fig. 1). While small crystals of the same mineral assemblage as in the LTB have formed in the middle portion resulting in small compositional changes, the bottom portion of the experiment remains largely similar in composition to the starting material. In contrast, the 34-day-long LTB experiment resulted in 5‰ $\delta^{18}O$ separation in the upper portion which ranged from fully to partially molten. This in itself is important as it shows that thermal diffusion of O in a dry melt results in significant isotopic fractionation with the sensitivity, Ω, for the molten and partially-molten part of this experiment being ~0.016‰/°C. This value is similar to the Ω determined from previous dry, 2 week-long Soret experiments (Kyser et al., 1998; Fig. 4), suggesting that a near steady state O isotopic redistribution has been achieved in the upper all melt section in 34 days.

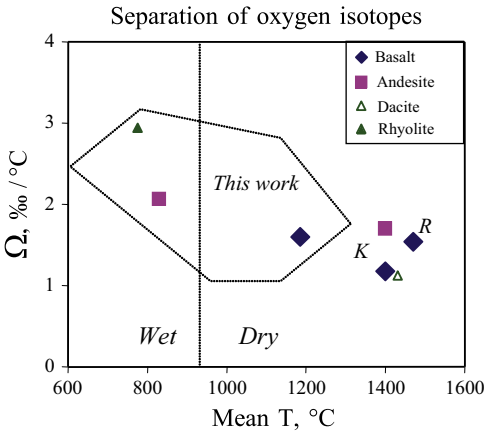

Fig. 4. Omega parameter for oxygen isotopes representing permil separation as a function of mean temperature of experiments of different composition, wet and dry. Experiments that reached steady state based on times series (Kyser et al., 1998, labeled K) and (Richter et al., 2009, labeled R) are also plotted. Notice that experiments of this study plot alongside with all-melt-steady-state experiments.

3.2. Wet experiments with andesite and rhyolites

In contrast to the dry basalt experiments, the wet experiments show a remarkable degree of compositional and isotopic redistribution throughout the experiments. The water distribution in the wet AGV and RGM experiments is fairly similar, with the majority (6–7 wt%) dissolved in the entirely molten upper portion of the experiments (Fig. 2). This water concentration is about 3 wt% less than that needed to saturate silicate melts at the pressure of these experiments (based on MELTS estimates above or Holtz et al., 2001 for generic silicic melts). The bulk water concentration decreases as the mode of melt decreases down temperature. In the cold bottom half of each experiment, the water distribution reflects the proportions of hydrous phases (micas and amphibole) present (Fig. 2). In detail the profiles are different: water concentration steadily decreases in the middle portion of the AGV experiment and then flattens out at 0.5 wt% in the crystalline, biotite and amphibole-bearing cold end. In the RGM experiment, the water profile is sigmoidal due to the presence of abundant muscovite at the cold end of the charge (accounting for 1.5–2 wt% total water) and the presence of plagioclase-rich layer in the middle of the charge (with 0.2–0.8 wt% bulk water). The short-term experiment MA-1 shows transitional behavior of H_2O, $\delta^{18}O$, and δD (Fig. 3).

$\delta^{18}O$ varies nearly linearly with temperature through both long-term wet experiments with the hot end isotopically lighter than the cold end with total offsets by 23–28‰ (Fig. 1). This occurs across the entire length of the charge, *regardless* of the large changes in crystallinity or composition across the capsules. The observed oxygen isotope profile in LTM-AGV is consistent with mass balance using the measured $\delta^{18}O$ values of the AGV-1 powder and water starting materials. We also performed triple-oxygen isotopic measurement on top and bottom of AGV

experiment (Table 1), and determined it to be mass-dependent within 2st dev ± 0.18‰ uncertainty of our measurements during this analytical session (fluorination, double-freezing, mass-spectrometry) and choice of exponent in $\Delta^{17}O$ definition (but see Sun and Bao (2011) for small deviations at low gas pressure experiment with pure O_2 gas).

The hydrogen isotopic measurements in LTM-AGV demonstrate a remarkable 144‰ range. However, the δD profile is distinct from the more linear $\delta^{18}O$ being flat and heavy (ca+20‰) in the crystal-rich, biotite and amphibole-bearing, water-poor cold end of the capsule, undergoing a steep isotopic gradient in the middle section, and finally flattening again with a light isotopic compositions in the upper melt-rich hot end of the charge. Notably, the shape of the δD profile mimics that of water concentration. The hydrogen isotopic distribution in this long-term, double capsule experiment are demonstrated to be robust because there is good mass balance for both O and H isotopes and water relative to the starting materials, and isotopic sensitivity of hydrogen is consistent with mass-dependent behavior based on other isotope systems (Fig. 4). In particular, the fact that isotopic variations of hydrogen are 8–10 times that of oxygen, similar to the relationship in the meteoric water line, suggests that it is the water molecule that is responsible for mass-dependent transport. The δD of the starting water added to the experimental charge is -43‰ (Fig. 1); integrating the wt% H_2O and δD across the run product yields a bulk δD of -42‰ to -48‰, overlapping the initial water value and suggesting that no water or preferential H_2 loss (affecting D/H) occurred during the experiment.

In the RGM experiment, TCEA analysis indicates water concentrations appropriate for the amount of water initially added indicating that water was overall retained during the RGM experiment. However, the inner capsule must have had a small leak, as peaks of Co and Cl, presumably from the $CoCl_2$ in the outer capsule, were discovered in the melt. Therefore, because the $AuPd_{25}$ capsule is impermeable to hydrogen but the Pt capsule is not, H was likely to have behaved as an open system resulting in overall heavy values of+100‰ δD throughout the capsule; these results are not further discussed. Hydrogen loss and isotopic fractionation toward heavier values during loss through Pt capsule walls is a well-known phenomenon (Richet et al., 1986; Graham et al., 1987). Nevertheless, given that the outer capsule remained intact, the results presented for molecular water, major elements and $\delta^{18}O$ distribution remain valid.

Lastly, the measurements of the two-endmember chips of LTM-AGV for δ^7Li (Table 1) also show a pronounced offset of 18.5‰, with lighter values at the hot end. This change is coupled to ~7 times decrease in elemental Li concentration (from 82 to 12 ppm) between the hot to cold ends respectively.

3.3. Short-term experiment MA-1

The magnitude of isotopic change in short term wet experiment is 18‰ for $\delta^{18}O$ and 70‰ for δD (Fig. 3), about one half of the values in long-term wet experiments. Most of these variations occur at the cold end. This short term experiment capture a transient state before attainment of steady state in the entire capsule. Rapid chemical and isotopic modification must occur at the cold end of the capsule. Based on H_2O and D/H mass-balance in the whole capsule, the glass must breakdown into minerals and a fluid that allows rapid transport and oxygen isotopic exchange throughout the cold end of the experiment. However, diffusion through the silicate melt at the hot end is relatively slower and thus no oxygen isotopic change has yet occurred in this part of the experiment, although D/H exchange is already seen. The transition from MA-1 (10 day) to a "steady state" RGM (25-day) or 66-day AGV experiments is likely caused by a rapid solution–reprecipitation of the melt/solid boundary and water diffusion into the melt. This should happen at estimated minimal 5×10^{-7} cm^2/s rates (see below) of hydrogen and water diffusion into the 850 °C melt (12 days over 7 mm distance). The observation that significant isotopic fractionation occurs within this experiment using hydrous glass argues that the large isotopic offsets in the long-duration wet experiments are not simply an artifact of the experimental set up of molecular water being added to powdered dry rocks.

4. Discussion

4.1. The leading role of solution–reprecipitation via fluid films in promoting isotope exchange in thermal gradient experiments

The progressive change in the relative proportion of minerals and melt, and bulk SiO_2 content[2] with position in the wet experiments (Fig. 1, Table 1) would seemingly present a complicated scenario for interpreting the isotopic signatures of thermal diffusion. Yet the smooth and simple $\delta^{18}O$ variations suggest that the oxygen isotope redistribution has achieved a near steady-state condition. Oxygen diffusion in wet melts is known to reflect diffusion of molecular H_2O through the melt with diffusivity being orders of magnitude higher than O in dry melts ($\sim10^{-7}$ cm^2/s, Zhang et al., 1991; Behrens et al., 2007). Oxygen diffusion with rates of $\sim10^{-7}$ cm^2/s can be deduced from 5 to 7 mm all-melt portions (Fig. 2) of our 25–66 day-long experiments. What is remarkable in the simplicity of the O isotope distribution is that even the colder, subsolidus crystal-rich ends at temperatures of 350–600 °C have developed significant gradients in $^{18}O/^{16}O$ even in short-term MA-1 experiment (Fig. 3). Given slow rates of intracrystalline oxygen diffusion through feldspar (10^{-22} m^2/s at ~550 °C, Graham and Elphick, 1990), rapid exchange of oxygen between fluid/melt and minerals must occur by solution–reprecipitation and recrystallization (Idlefonse and Gabis, 1973). This is also consistent with calculations showing that silicate minerals undergo dissolution–reprecipitation in supercritical H_2O in a temperature gradient (Oelkers et al., 2007).

The mineral–melt (or mineral–fluid) isotopic exchange is very rapid and $\delta^{18}O$ at each location in the capsule reflects the thermally-migrated ^{18}O, not that of the particular mineral phases at that location. The observed changes in $\delta^{18}O$ suggest that thermal redistribution overwhelms any mineral-melt fractionation effects. For example, an offset to lower $\delta^{18}O$ of the bulk sample chip containing ~20% magnetite might be expected because magnetite has the largest mineral–silicate melt fractionation factor ($\Delta^{18}O_{Mt-melt}$ of ~-6‰ at the inferred temperature, e.g., Eiler, 2001; Bindeman, 2008); however, no such offset can be observed in the middle of AGV experiment (Fig. 2). Similarly, the bottom almost pure quartz sample from both AGV and RGM experiments have the heaviest isotope signature (+18‰) with larger than equilibrium $\Delta^{18}O$(Qz–WR) value for any section of the capsules at given temperature. Given the bulk nature of our

[2] Huang et al., 2009 documented that the lower (colder) portion of the AGV experiment converted to a granitic bulk composition, and we discovered nearly pure quartz at the end of this experiment. Similarly, the RGM experiment shows considerable enrichment in silica content at the bottom. Thus, common trait of both experiments is transport of silica down the temperature gradient leading to increasing SiO_2 at the cold end of the gradient. This is most easily explained by the strong temperature dependence of quartz solubility in melts and hydrous fluids (Watson and Wark, 1997; Burchard et al., 2011). An overarching observation from these 5 experiments (3 wet, 2 dry) is that only the wet experiments show the strong silica enrichment at the low temperature end. This corresponds with the full resetting of the $\delta^{18}O$ of the bulk material—both reflecting the role of water dissolved in melt in a temperature gradient.

measurements, we cannot estimate the $\delta^{18}O$ value of each phase at a given T. In situ isotopic analysis of coexisting phases could potentially provide important temperature information, using established isotope thermometers, although this may be difficult analytically at present given small crystal sizes, uncertainties related to matrix effects and difficulties in obtaining a flat surfaces for ion probe analyses.

The hydrogen isotopic measurements in LTM-AGV (Fig. 2) are the first to demonstrate the role of thermal diffusion in isotopically-fractionating hydrogen in silicate melts with δD spanning a remarkable 144‰ range. The difference between the $\delta^{18}O$ and δD profiles reflect the importance of the melt–mineral and mineral–mineral isotopic fractionation on δD; for instance, hydrogen isotopes partition between OH and H_2O molecular sites with isotopic differences of 60‰ at these temperatures (Dobson et al., 1989). Indeed, the 0.5 wt% bulk water content of the lower half of LTM-AGV almost entirely reflects the OH-bearing minerals amphibole and biotite; notably, these minerals preferentially take in H over D with the magnitude of mineral–melt fractionation getting larger as temperature decreases. Thus, because hydrogen is held in these minerals, lower offsets in δD across the temperature gradient than would be expected for thermal diffusion likely occur.

The observation of δD and $\delta^{18}O$ changing throughout LTM-AGV contrasts with profiles for Mg and Fe isotope ratios which only show significant changes from the starting material in the upper half of the charge where visible amounts of quenched melt occur (Huang et al., 2009). The simplest explanation for the different behavior of isotopic systems is that molecular water moves freely through the solid material even at the low temperature end but that Mg and Fe do not, presumably because their concentrations in this melt/fluid are too low to quantitatively effect the isotopic composition of the crystalline lower half. The 18.5‰ offset in δ^7Li across LTM-AGV shows that water-soluble elements do move through the entire charge. Li also demonstrates a $\Delta M/M$ mass dependent isotopic variation (Table 1, Fig. 1) consistent with other isotope systems (Fig. 4).

The smooth bulk $\delta^{18}O$ profile can only be explained if the formation of the steady-state mineral assemblage was caused by fluid-assisted solution–reprecipitation of transient mineral assemblages throughout the experimental run. This likely involved mineral-reaction fronts which not only changed grain size and modes but also led to temporal changes in the assemblage present (e.g. quartz zone substituting muscovite). It is obvious that such a dramatic change should redistribute the major elements—oxygen, not to mention other elements. We attribute the rapidity of this solution–reprecipitation process to the effect of thin films of supercritical water (melt) solutions (e.g. Putnis and Putnis, 2007).

4.2. Constraining the minimum rate of thermal diffusion and isotopic resetting

Our results with wet subsolidus samples are broadly consistent with previous results of dry oxygen isotopic fractionation by thermal diffusion in silicate melts. This argues that the water-bearing experiments provide an extension of the same thermal diffusion process into the realm of a solid material reacting with hydrous fluid by solution–reprecipitation, and exchanging mass through it. Fig. 5 shows our results along with data from Kyser et al. (1998) and Richter et al. (2008), which represent Soret experiments at higher mean temperature. The magnitude of thermal isotopic separation of oxygen (Ωo) for LTB dry basalt is similar to these previous studies. The Ωo for the two long duration wet experiments of this study not only approach but exceed those measured previously in all-melt experiments (Fig. 5)

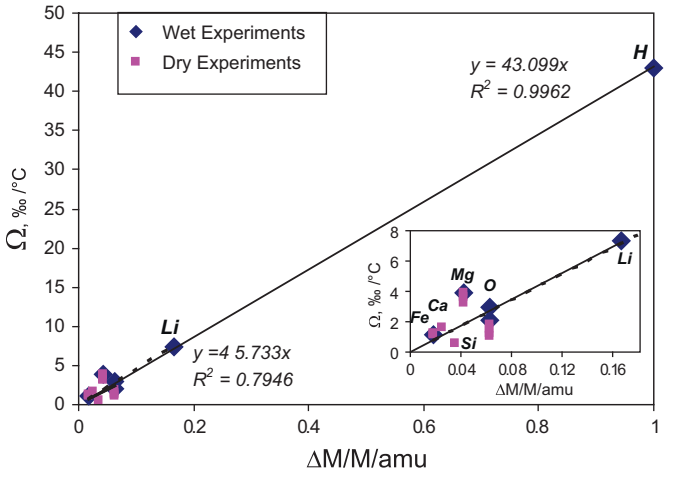

Fig. 5. Omega parameters as a function of isotope identity expressed through relative mass difference $(M_{heavy}-M_{light})/M_{light}$/amu for wet experiments of this study as compared to dry Soret experiments of Lesher and Walker (1991), Kyser et al. (1998), Richter et al. (2008, 2009), see supplementary material for compiled data. Inset shows blow up of heavier mass elements (all except H) that yield the same slope of fit (dashed line). Notice the strong positive correlation of omegas for wet experiments and scatter for dry experiments.

that have been shown through time series results to reflect steady state (Kyser et al., 1998). Thus, our long-term water-bearing experiments can also be argued to have attained steady-state, while the 10-day-long MA1 experiment has not. This allows us to constrain a minimum diffusion coefficient relevant to generating the observed isotopic signature.

We can estimate (within one order of magnitude) the values of the "effective isotopic sorting diffusion coefficient" (D) by taking the total experimental duration, t, the length of the capsule, x, and assuming a $D=X^2/t$ relationship. Estimated this way, D is between the 2×10^{-5} to 2×10^{-6} cm^2/sec across the entire (melt and solid) portion of the LTM-AGV. A second estimate for the all-solid lower half of the capsule of the RGM experiment, 0.7 cm in length and with a median temperature of 550 °C range from 2×10^{-6} to 2×10^{-7} cm^2/s. These are extraordinarily fast estimates of diffusive transport suggestive of mass transfer through fluid phase. We therefore argue that transport across temperature gradient involves a solution–reprecipitation process that is catalyzed by the presence of the coexisting supercritical, pegmatite-like hydrous fluid/melt.

4.3. Stable isotopic evidence of pegmatite-like Hydrous fluid

Dramatic modifications of $\delta^{18}O$ and δD throughout even the nominally subsolidus cold end of the wet experiments provide the most direct evidence that a water-rich, pegmatite-like fluid–melt described by Tuttle and Bowen (1958), advocated by Huang et al. (2009), and found by Sirbescu and Nabelek (2003) in nature, has caused chemical transport and isotopic exchange *throughout the material* at the cold end of a temperature gradient. Furthermore, Huang et al. (2009) and Lundstrom (2009) provide detailed compositional lines of evidence that the transport of material through LTM-AGV (and by analogy the RGM experiment here), that this fluid has properties of hydrous peralkaline silicate melt down to temperatures as low at 350 °C (Tuttle and Bowen, 1958). The compositional and isotopic results here support the inference of a continuum of melt to fluid–melt and then to hydrothermal-like solutions in the wet experiments. The presence of newly-grown hydrous minerals in the cold ends of these charges demonstrates the role of this fluid in affecting crystallization of new phases. The wholesale resetting of δD and $\delta^{18}O$ within the

wet experiments provides primary evidence for a continuous transition from silicate melt to hydrous fluid and that this fluid-melt which can in turn be tied to the dramatic compositional changes observed in the wet experiments.

4.4. Does water promotes greater isotope separation?

Regardless of second-order complexities in isotopic profiles, the direction and magnitude of $\delta^{18}O$, δD, $\delta^{7}Li$, and previously reported Mg and Fe isotopes for LTM-AGV are fully consistent with isotopic fractionation by thermal diffusion: light isotopic compositions are consistently found at the hot end of the gradient while heavy ratios are found at the cold end (cf. Kyser et al., 1998; Richter et al., 2009 for all-melt systems). Fig. 5 illustrates a simple linear correlation of $\Delta M/M$ vs. $\Delta\delta$ in our experiments. The correlation suggests isotope separation is very simply related to the relative mass difference with little or no regard to the identity of isotopes, other components in the melt or even the presence or absence of crystals.

Comparison of our results with previous all -melt (Soret) studies of oxygen isotope redistribution during anhydrous thermal diffusion shows that the magnitude of the oxygen isotope separation *increases with increasing* water content (Fig. 4). The simplest explanation for this behavior is that the thermal diffusion fractionation depends on an "effective mass" of a diffusing molecule carrying the isotope of interest. For instance, in a dry melt, O is primarily bonded to Si and its diffusive hopping ability will depend in part on its neighbors-its effective mass is that of SiO. In the wet experiments, O is dominantly moving by diffusion attached to H (molecular H_2O) such that its effective mass (where the isotope signature is produced) is close to that of O (H_2O). Watkins et al. (2011) observed that the magnitude of kinetic isotope fractionation is dependent on the ratio of diffusion coefficients for the diffusing cation to that of silica. They observed that the greatest kinetic isotope fractionation occurred when the diffusion coefficients differed most strongly and explained it by the size of the diffusing particle. In our case, the presence of hydrothermal fluid (or "pegmatitic" melt) at the cold end of the wet experiments led to a greater proportion of non-bridging, water-associated oxygen atoms that facilitated greater isotope fractionation than in the dry melt case. This leads to greater separation by thermal diffusion as shown by the Omega parameter of the water bearing experiments being roughly double that of dry experiments (Fig. 4).

Lacks et al. (2012) propose that the thermal diffusion isotopic fractionation is purely mechanical, being related to momentum differences of isotopes (after Enskog, 1911); in essence, when heavy isotopes diffusively hop from higher to lower temperature, they exceed a threshold momentum that results in their net movement toward the cold end causing it to be isotopically heavy (with the hot end correspondingly light). This explanation is consistent with our observations in that the isotopic profiles of elements (O, H, Li, Mg, Fe) are decoupled from the chemical fluxes backed out from the compositional changes in the experiments (Fig. 6). According to Lacks et al. (2012), isotopic fractionation scales with the relative mass difference. In Fig. 7, instead of normalizing the isotopic offsets by $(m_1-m_2)/(m_1+m_2)$, we have simply examined delta versus the normalized temperature and regressed slopes. Based on this mass relationship, the δD slope should be $\sim 5\times$ that of $\delta^{18}O$ and $4\times$ that of $\delta^{7}Li$. While there are many assumptions and caveats in the data including the definition of "effective mass differences", the change in slopes decreases in expected order (H→Li→O) with the magnitude of change within reasonable range of prediction.

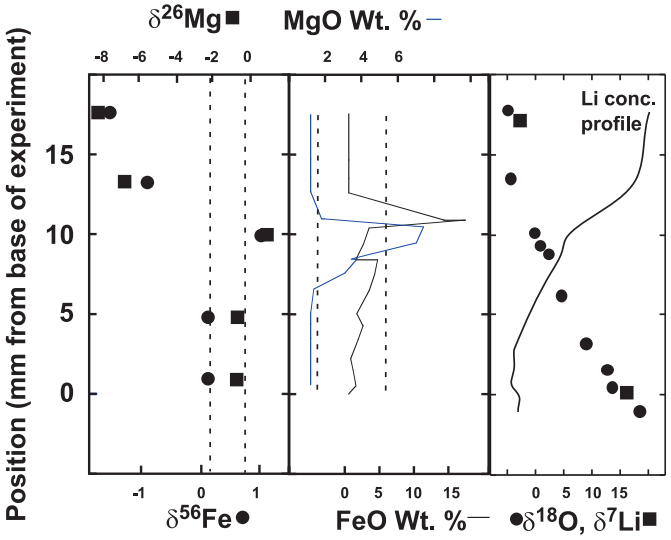

Fig. 6. Isotopic ratio and concentration profiles for Mg, Fe, Li and O in the LTM-AGV experiment (Mg and Fe isotopic data along with concentration profiles from data in Huang et al. (2009)). Dashed lines show initial MgO and FeO profiles in experiment. Li initial is partially unknown as a significant portion of Li came from contamination by the capsule (see Huang et al., 2009). Note that the molar change in O concentration within the experiment is negligible with less than a 10% increase occurring in the bottom due to the granitic bulk composition. The data show the complete independence of the isotopic profiles from the mass redistribution (chemical fluxes) occurring during the experiment. This independence reinforces the conclusion of Lacks et al. (2012) that the isotopic effect is mechanical in origin and decoupled from chemical effects of redistribution.

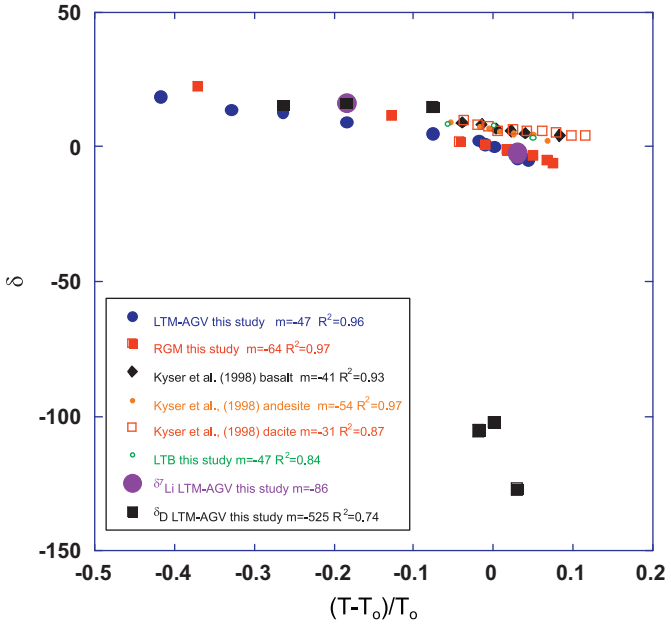

Fig. 7. Isotopic offsets vs. $T-T_o/T_o$ for LTM-AGV, LTB and experiments of Kyser et al., (1998). Slopes for all systems and experiments are given in legend along with R^2. Based on Lacks et al. (2012), the slope for δD should be 4x that of $\delta^{7}Li$ and 5x that of $\delta^{18}O$. The relative slope difference within LTM-AGV experiment is consistent with this prediction. Note the more negative slopes of $\delta^{18}O$ for the wet experiments relative to the dry ones, consistent with the smaller "effective" mass of O in these experiments (see text).

4.5. Implications

The immediate implication of our results is a word of caution to nominally-isothermal, wet and long-term isotope exchange

experiments. Minor T gradients of several tens of degrees may imprint permil-scale fractionations.

The magnitude of isotope and chemical separation in temperature gradient does not depend on the gradient but rather on the absolute temperature difference between point A and B. Thus, results from our experiments with gradients of hundreds of °C per cm can quantitatively capture the magnitude of expected chemical and isotopic modification in nature, if given enough time. When scaled to natural environments (as x^2/D), the time required to achieve steady state becomes progressively larger, with geologically-relevant length scales of centimeters to meters increasing proportional to the square of distance.

Through comparison of the H, Li and O isotopic separations in wet and dry silicate temperature gradient experiments, we have shown the profound effect that dissolved water in silicate melt in a temperature gradient has on redistributing mass and imparting a thermal diffusion isotopic signature on solid materials. An implication of this experimental result (if it holds for nature) is that isotopic redistribution can occur along margins of plutons, and in hydrothermal systems if temperature gradients are sustained, and convective rehomogenization is suppressed (Fig. 8). Given the long duration of plutons that indicate continuous input of heat (e.g. Coleman et al., 2004; Annen et al., 2006), sustained temperature gradients could lead to significant (if even localized) isotopic changes due to thermal diffusion.

We demonstrated above that the rates of modification in the wet experiments occur with "effective thermal diffusion" coefficients ranging from of 10^{-5} to 10^{-7} cm^2/s for oxygen, implying significantly faster transport rates than originally argued by Bowen (1921). Furthermore, given that newly-determined high pressure thermal diffusivities are half those previously thought (now: ca. 0.5×10^{-2} cm^2/s, Whittington et al., 2009), chemical transport within a sustained temperature gradient would only take 10^2–10^4 times longer than dissipation of heat, not 10^8–10^{10} times longer as previously advocated by Bowen (1921).

Thus, if a temperature gradient is maintained in a pluton's contact or roof pendant containing just a trace of interstitial water, a prediction of direction and magnitude of isotopic exchange can be made (high-δ^{18}O, high Si at cold end, low-δ^{18}O toward the melt, Fig. 8) with even some ability to infer rates. For instance, if thermal migration occurred over 10 m distance with D of 10^{-5}–10^{-6} cm^2/s (as advocated above), it will take $\sim3\times10^3$ to 3×10^4 years to achieve steady state (and less time for partial isotopic change). Such durations are likely similar in magnitude to contact aureoles for plutons, given current ideas of incremental emplacement (Glazner et al., 2004). If temperature gradients are maintained over tens of meters, this may explain high-δ^{18}O values of some roof pendants above Sierra Nevada granites (Hanson et al., 1993).

While the above arguments apply to oxygen and other major elements, redistribution of hydrogen and lithium appear to occur many orders of magnitude faster, *comparable* to rates of heat diffusion. We further suggest that remarkably large isotopic separation of hydrogen isotopes in a thermal gradient that we first measured, coupled with its intrinsically fast diffusion in melts and fluids can be used to test and potentially explain D/H systematics of degassing magmas, rims on pillow lavas, and fumarolic gases. At $D=10^{-4}$ cm^2/s, thermal diffusion alone is capable of achieving a $\sim$30‰ separation in 150 °C temperature gradient over 300 years over 10 m distance. This is comparable to rates of heat diffusion. A global survey of fumarolic gasses does provide a picture of universally heavier D/H values in fumarolic waters ($-20\pm10+10$‰, Giggenbach, 1992) over primary magmatic water (ca -65 ± 15‰), consistent with isotope redistribution in the temperature field (e.g., Fig. 8).

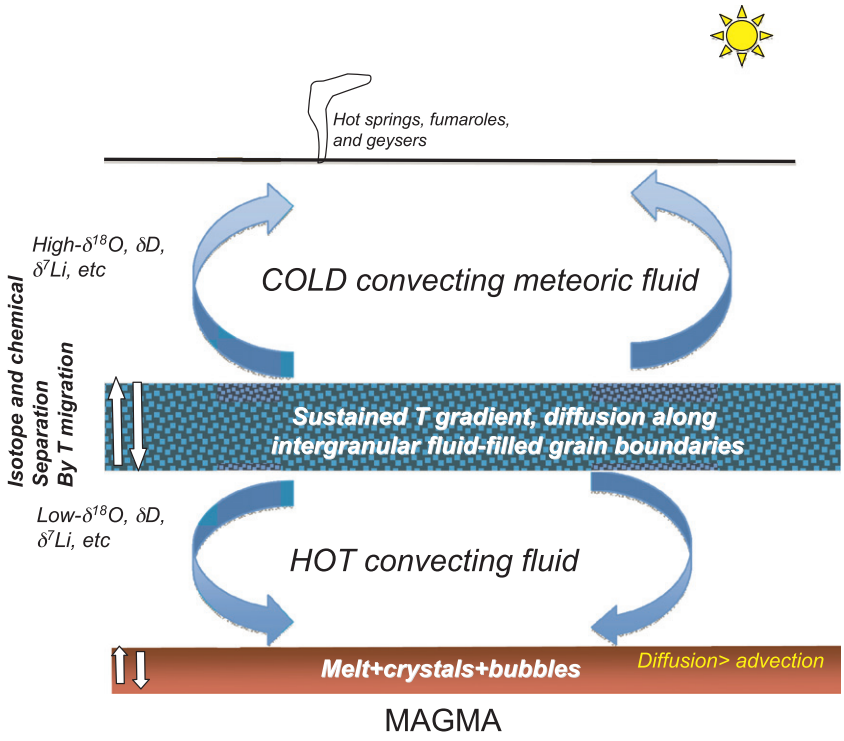

Fig. 8. A cartoon illustrating magma-hydrothermal transition and showing two spatial areas where temperature gradients may be sustained for long stretches of time to induce isotope (and chemical) separation of fast-diffusing elements by thermal redistribution. The sense of predicted isotope redistribution is shown. Transport through water-filled impermeable barite-precipitation transition zone (upper box) within hydrothermal system may be much faster than diffusion through a near interstitial melt near solidus (lower box). In order for isotope effects to be preserved, diffusion should be faster and not be followed by convective (advective) rehomogenization. Subsequent melting of rocks altered this way may generate isotopically-diverse batches.

Although not a subject in this paper, we can also foresee how slow and putative advection may accelarate achieving maximum thermal isotopic effects, similar to what is occurring in industrial applications aimed at thermal isotope separation (Grew and Ibbs, 1952; Vasaru et al., 1969).

The results here demonstrate the profound behavior of magmatic water in a temperature gradient to transport, react and exchange with solids. The presence of water allowed achievement of a steady state isotopic redistribution in almost entirely crystalline material at $<400\,^{\circ}C$, all occurring over significantly faster timescales than diffusion in a high temperate silicate melt. The implications of this process could be far reaching including blurring the boundary between the traditions of igneous and metamorphic petrology and providing new insights into the magmatic-hydrothermal transition (Fig. 8) or the low- and high-$\delta^{18}O$ (and δD) signatures in magmas and rocks. Examinations of stable isotope variations from igneous contacts with country rock or within cooling subvolcanic extrusive bodies or roof pendants could prove fruitful. We further speculate that large (and disequilibrium? Taylor, 1974) ΔD(mantle-hydrosphere) isotope fractionation can partly be explained by the effects of thermally-fractionating hydrogen. We do not doubt, however, that fractional crystallization and partial melting are the chief petrogenetic processes.

Acknowledgments

NSF grants EAR-0805972 and 1019632 supported this work. We thank Yan Liang, Alan Rempel, and an anonymous reviewer for helpful comments, Bill McDonough and Roberta Rudnick for Li isotopic measurements, and Erwan Martin and Jim Palandri for help in calibrating D/H in glass protocols.

Appendix A. Supporting information

Supplementary data associated with this article can be found in the online version at http://dx.doi.org/10.1016/j.epsl.2012.12.037.

References

Annen, C., Scaillet, B., Sparks, R.S.J., 2006. Thermal constraints on the emplacement rate of a large intrusive complex; the Manaslu Leucogranite, Nepal Himalaya. J. Petrol. 47, 71–95.

Barth, T.F.W., 1962. Theoretical Petrology, 2nd Edition Wiley, New York. (416 pp).

Behrens, H., Zhang, Y.X., Leschik, M., Wiedenbeck, M., Heide, G., Frischat, G.H., 2007. Molecular H_2O as carrier for oxygen diffusion in hydrous silicate melts. Earth Planet. Sci. Lett. 254, 69–76.

Bindeman, I.N., 2008. Oxygen isotopes in mantle and crustal magmas as revealed by single crystal analysis. Rev. Mineral. Geochem. 69, 445–478.

Bindeman, I.N., Kamenetsky, V.S., Palandri, J., Vennemann, T., 2012. Hydrogen and oxygen isotope behavior during variable degrees of upper mantle melting: example from the basaltic glasses from Macquarie Island. Chem. Geol. 310–311, 126–136.

Boudreau, A.E., 2003. IRIDIUM—a program to model reaction of silicate liquid infiltrating a porous solid assemblage. Comput. Geosci. 29, 423–429.

Bopp, 2010. The Isotope Geochemistry of Uranium: Igneous Petrology, Ore Deposits and Groundwater Contamination. Ph.D. Thesis. University of Illinois at Urbana Champaign.

Bowen, N.L., 1921. Diffusion in silicate melts. J. Geol. 29, 295–317.

Buchwatd, V.F., Kjer, T., Tborsen, K.A., 1985. Thermal migration I: or how to transport iron sulfide in solid iron meteorites. Meteoritics 20, 617–618.

Burchard, M., Maresch, W.V., Fockenberg, T., Doltsinis, N.L., Adeagbo, W.A., 2011. Modelling high-pressure aqueous fluids in the system $CaO–SiO_2–H_2O$: a comprehensive semi-empirical thermodynamic formalism. Eur. J. Mineral. 23, 409–424, http://dx.doi.org/10.1127/0935-1221/2011/0023-2106.

Campbell, I.H., Taylor, S.R., 1983. No water, no granites–no oceans, no continents. Geophys. Res. Lett. 10, 1061–1064.

Dobson, P.F., Epstein, S., Stolper, E.M., 1989. Hydrogen isotope fractionation between coexisting vapor and silicate glasses and melts at low pressure. Geochim. Cosmochim. Acta 53, 2723–2730.

Dominguez, G., Wilkins, G., Thiemens, M.H., 2011. The Soret effect and isotopic fractionation in high-temperature silicate melts. Nature 473, 70–72.

Eiler, J., 2001. Oxygen isotope variations of basaltic lavas and upper mantle rocks. In: Valley, J.W., Cole, D.R., (Eds.), Stable Isot. Geochem., Rev. Mineral. Geochem. 43, 319–364.

Enskog, D., 1911. Remarks on a fundamental equation in kinetic gas law. Phys. Z. 12, 533–539.

Hanson, R.B., Sorensen, S.S., Barton, M.D., Fiske, R.S., 1993. Long-term evolution of fluid-rock interactions in magmatic arcs: evidence from the Ritter Range pendant, Sierra Nevada, California, and numerical modeling. J. Petrol. 34, 23–62.

Hildreth, W., 1981. Gradients in silicic magma chambers: implications for lithospheric magmatism. J. Geophys. Res. 86, 10153–10192.

Huang, F., Lundstrom, C.C., Glessner, J., Ianno, A., Boudreau, A., Li, J., Ferre, E.C., Marshak, S., DeFrates, J., 2009. Chemical and isotopic fractionation of wet andesite in a temperature gradient: experiments and models suggesting a new mechanism of magma differentiation. Geochim. Cosmochim. Acta 73, 729–749.

Huang, F., Chakraborty, P., Lundstrom, C.C., Holmden, C., Glessner, J.J.G., Kieffer, S.W., Lesher, C.E., 2010. Isotope fractionation in silicate melts by thermal diffusion. Nature 464, 396–399.

Holtz, F., Johannes, W., Tamic, N., Behrens, H., 2001. Maximum and minimum water contents of granitic melts generated in the crust: a reevaluation and implications. Lithos 56, 1–14.

Giggenbach, W.F., 1992. Isotopic shifts in waters from geothermal and volcanic systems along convergent plate boundaries and their origin. Earth Planet. Sci. Lett. 113, 495–510.

Ghiorso, M.S., Sack, R.O., 1995. Chemical mass-transfer in magmatic processes IV. A revised and internally consistent thermodynamic model for the interpolation and extrapolation of liquid–solid equilibria in magmatic systems at elevated temperatures and pressure. Contrib. Mineral. Petrol. 119, 197–212.

Glazner, A.F., Bartley, J.M., Coleman, D.S., Gray, W., Taylor, R.Z., 2004. Are plutons assembled over millions of years by amalgamation from small magma chambers? GSA Today 14, 4–11.

Graham, C.M., Elphick, S.C., 1990. Diffusion in feldspar in presence of water a reexamination of the role of hydrogen in Al-Si interdiffusion in feldspars. Contrib. Mineral. Petrol. 104, 481–491.

Graham, C.M., Viglino, J.A., Harmon, R.S., 1987. Experimental-study of hydrogen-isotope exchange between aluminous chlorite and water and of hydrogen diffusion in chlorite. Am. Mineral. 72, 566–579.

Grew, K.E., Ibbs, T.L., 1952. Thermal Diffusion in Gases. Cambridge University Press (252 pp).

Idlefonse, J.-P., Gabis, V., 1973. Experimental study of silica diffusion during metasomatic reactions in the presence of water at 550 C and 1000 bars. Geochim. Cosmochim. Acta 40, 297–303.

Kyser, T.K., Lesher, C.E., Walker, D., 1998. The effects of liquid immiscibility and thermal diffusion on oxygen isotopes in silicate liquids. Contrib. Mineral. Petrol. 133, 373–381.

Lacks, D.J., Goel, G., Bopp, C.J., VanOrman, J.A., Lesher, C.E., Lundstrom, C., 2012. Isotope fractionation by thermal diffusion in silicate melts. Phys. Rev. Lett. 108, http://dx.doi.org/10.1103/PhysRevLett.108.065901, Article Number: 065901.

Lesher, C.E., Walker, D., 1991. Thermal diffusion in petrology. In: Diffusion, Atomic Ordering, and Mass Transport. In: Ganguly, J. (Ed.), Advances in Physical Geochemistry, 8. Springer–Verlag, New York, pp. 396–451.

Lesher, C.E., Walker, D., 1988. Cumulate maturation and melt migration in a temperature gradient. J. Geophys. Res. B9, 10295–10311.

Lesher, C.E., Walker, D., 1986. Solution properties of silicate liquids from thermal diffusion experiments. Geochim. Cosmochim. Acta 50, 1397–1411.

Lundstrom, C.C., 2009. Hypothesis for origin of convergent margin granitoids and Earth's continental crust by thermal migration zone refining. Geochim. Cosmochim. Acta 73, 5709–5729.

Nolan, G., Bindeman, I., 2013. Experimental investigation of rates and mechanisms of isotope exchange (O, H) between volcanic ash and isotopically-labeled water. Geochim. Cosmochim. Acta, http://dx.doi.org/10.1016/j.gca.2013.01.020, in press.

Oelkers, E.H., Putnis, C.V., Putnis, A., 2007. Do fluids flow through or around mineral grains? Geochim. Cosmochim. Acta 71, A729.

Onsager, L., 1931. Reciprocal relations in irreversible processes I. Phys. Rev. 37, 405–426.

Putnis, A., Putnis, C.V., 2007. The mechanism of reequilibration of solids in the presence of a fluid phase. J. Solid State Chem. 180, 1783–1786.

Richet, P., Roux, J., Pineau, F., 1986. Hydrogen isotope fractionation in the system H_2O liquid $NaAlSi_3O_8$—new data and comments on D/H fractionation in hydrothermal experiments. Earth Planet. Sci. Lett 78, 115–120.

Richter, F.M., Watson, E.B., Mendybaev, R., Dauphas, N., Georg, B., Watkins, J., Valley, J.W., 2009. Isotopic fractionation of the major elements of molten basalt by 210 chemical and thermal diffusion. Geochim. Cosmochim. Acta 73, 4250–4263.

Richter, F.M., Watson, E.B., Mendybaev, R., Janney, P.E., 2008. Magnesium isotope fractionation in silicate melts by chemical and thermal diffusion. Geochim. Cosmochim. Acta 72, 206–220.

Sirbescu, M.L.C., Nabelek, P.I., 2003. Crustal melts below 400 degrees C. Geology 31, 685–688.

Soret, C., 1879. Sur l'état d'équilibre que prend au point de vue de sa concentration une dissolution saline primitivement homohéne dont deux parties sont portées à des températures différentes. Arch. Sci. Phys. Nat. 2, 48–61.

Sun, T., Bao, H., 2011. Non-mass-dependent O-17 anomalies generated by a superimposed thermal gradient on a rarefied O-2 gas in a closed system. Rapid Commun. Mass Spectrom. 25, 20–24, http://dx.doi.org/10.1002/rcm.4825.

Taylor, H.P., 1974. The applications of oxygen and hydrogen isotope studies to problems of hydrothermal alteration and ore deposition. Econ. Geol. 69, 843–883.

Teng, F.-Z., Rudnick, R.L., McDonough, W.F., Wu, F., 2009. Lithium isotopic systematics of A-type granites and their mafic enclaves: further constraints on the Li isotopic composition of the continental crust. Chem. Geol., http://dx.doi.org/10.1016/j.chemgeo.2009.02.009.

Tuttle, O.F., Bowen, N.L., 1958. Origin of granite in the light of experimental studies in the system $NaAlSi_3O_8$–$KAlSi_3O_8$–SiO_2–H_2O. Geol. Soc. Am. Mem. 74.

Vasaru, G., Muller, G., Reunhold, G., Fodor, T., 1969. The thermal Diffusion Column: Theory and Practice With Particular Emphasis on Isotope Separation. Veb Deutscher Verlag, Berlin.

Walker, D., DeLong, S.E., 1982. Soret separation of mid-ocean ridge basalt magma. Contrib. Mineral. Petrol. 79, 231–240.

Walker, D., Jurewicz, S., Watson, E.B., 1988. Adcumulus dunite growth in a laboratory thermal gradient. Contrib. Mineral. Petrol 99, 306–319.

Watkins, J., DePaolo, D.J., Ryerson, F., Peterson, B., 2011. Influence of liquid structure on diffusive isotope separation in molten silicates and aqueous solutions. Geochim. Cosmochim. Acta 75, 3103–3118.

Watson, E.B., Wark, D.A., 1997. Diffusion of dissolved SiO_2 in H_2O at 1 GPa, with implications for mass transport in the crust and upper mantle. Contrib. Mineral. Petrol. 130, 66–80.

Watson, E.B., Price, J.D., 2002. Kinetics of the reaction $MgO + Al_2O_3 > MgAl_2O_4$ and AlMg interdiffusion in spinel at 1200 to 2000 degrees C and 1.0 to 4.0 GPa. Geochim Cosmochim Acta 66, 2123–2138.

Watson, E.B., Wark, D.A., Price, J.D., Van Orman, J.A., 2002. Mapping the thermal structure of solid media pressure assemblies. Contrib. Mineral. Petrol. 142, 640–652.

Whittington, A.G., Hofmeister, A.M., Nabelek, P.I., 2009. Temperature-dependent thermal diffusivity of the Earth's crust and implications for magmatism. Nature 458, 319–321.

Zhang, Y., Stolper, E.M., Wasserburgh, G.I., 1991. Diffusion of multi-specied components and its role in oxygen and water transport in silicates. Earth Planet. Sci. Lett. 103, 228–240.